CHAPTER 4

EXPERIMENTAL METHODOLOGY

The purpose of this Chapter is to provide a brief description of the primary apparatus and procedures which were used to perform the experimental measurements in the present study. The first Section gives the characteristics of the experimental apparatus; there are a flow system, a particulate-free air filter, a particle generator, an adjustable DC high voltage power supply, an electrometer, and a scanning electron microscope. The experimental test procedures of the charger, the classifier and the electrometer are described in the last Section.

4.1 Experimental Apparatus

This Section describes the experimental apparatus which were used to perform the experimental measurements in this study.

4.1.1 Flow system

Aerosol and sheath air flows were regulated and controlled by means of thermal mass flow meters and controllers. In the present study, commercial gas mass flow controllers (GFC), Dwyer model GFC-1111 and GFC-1142, were used. Figure 4.1 shows a picture of a Dwyer gas mass flow controller. In the configuration which was used, it has a flow rate range of 0 to 15 l/min for model GFC-1111, and 0 to 100 l/min for model GFC-1142 respectively, an accuracy of ± 1.5 % full scale, including linearity for gas temperatures ranging from 15° C to 25° C and pressures of 0.35 to 4.1 bar, and a response time of 300 ms time constant; approximately 2 s to within ± 2 % of set flow rate for 25 % to 100 % full scale. The vacuum pump was used to deliver the aerosol and sheath air flows into the classifier column. In the present study, the dry running rotary vane vacuum pump, Busch model SV 1003, was used. It has an ultimate pressure of 0.15 bar, and a nominal displacement volume rate of 3 m^3/h. A picture of the rotary vane vacuum pump is shown in Figure 4.2. For the connecting tube system, the polyethylene tubing (5 mm I.D. × 8 mm O.D.) was used in this system.

4.1.2 Particulate-Free Air Filter

A high efficiency particulate-free air (HEPA) filter, Pall HEPA capsule model 12144, was used to remove any particles, the first filter was placed upstream of the sheath air flow controller and the second filter was placed downstream of the classifier column in front of the total flow controller. It has a filtration efficiency of 99.97% retention of 0.3 μm for air/gas. Figure 4.3 shows a picture of the HEPA filter.

4.1.3 Particle Generator

In all the experiments reported in this thesis, the combustion aerosol generator (CAG) was employed to produce a polydisperse aerosol. Figure 4.4 shows a schematic layout of the main component of the CAG for the production of ultrafine carbonaceous particles. Polydisperse aerosols were produced by a laminar diffusion burner with a kerosene fuel in the nominal "presooting" condition. Under normal conditions, the vast majority of soot generated by the flame would be oxidized, giving a very low particle number concentration.

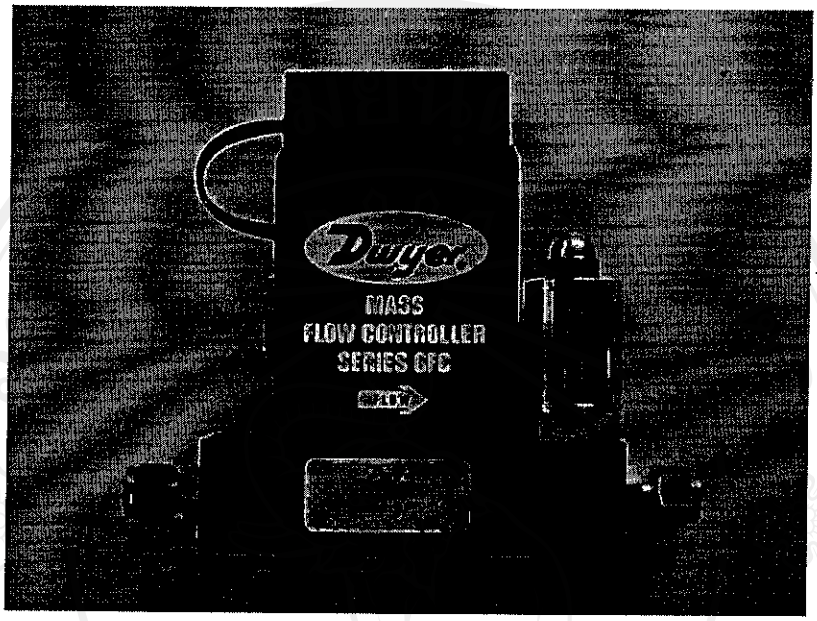

Figure 4.1 A picture of the Dwyer gas mass flow controller.

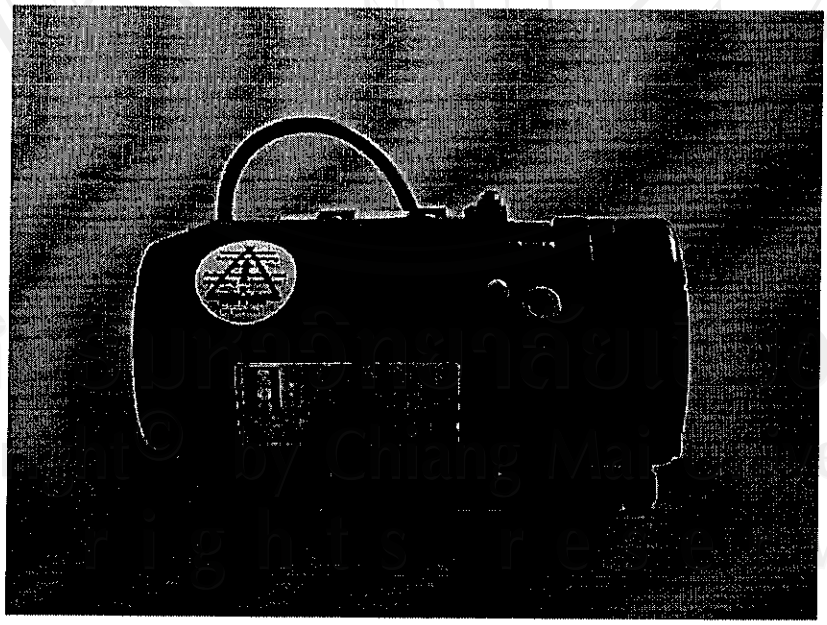

Figure 4.2 A picture of the rotary vane vacuum pump.

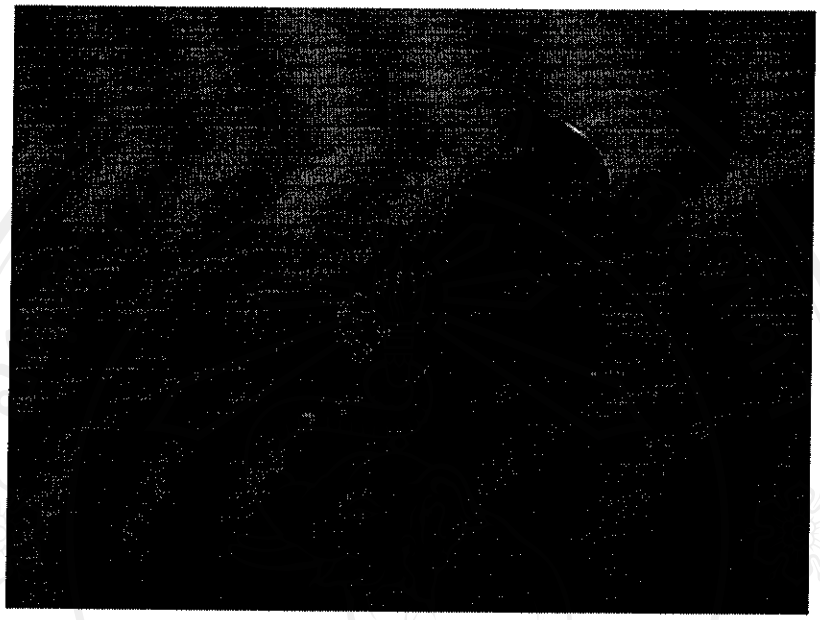

Figure 4.3 A picture of the high efficiency particulate-free air (HEPA) filter.

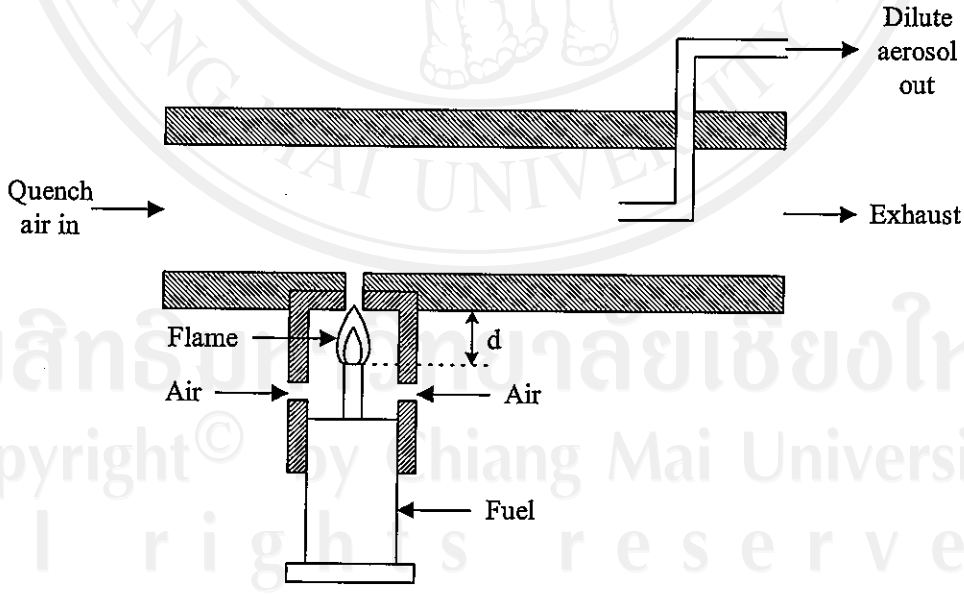

Figure 4.4 Schematic layout of the combustion aerosol generator (CAG).

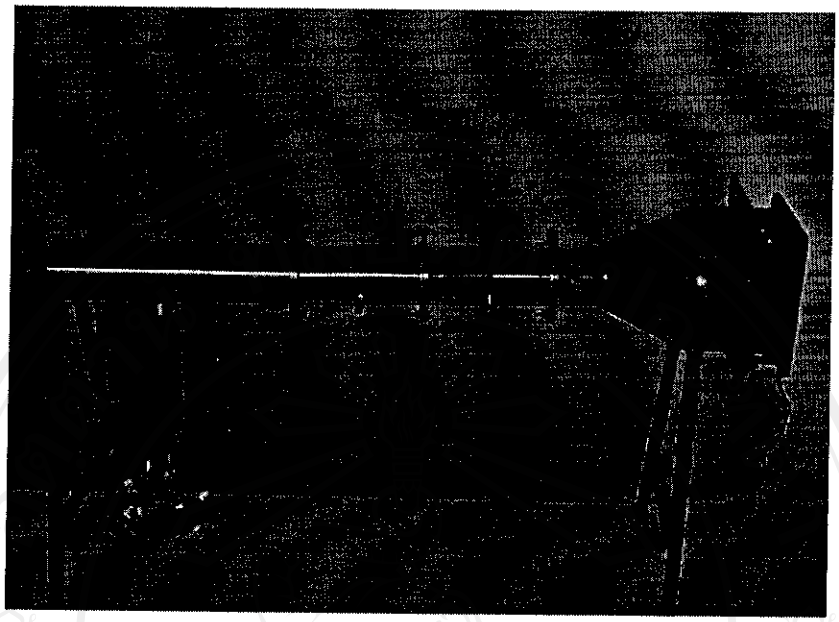

Figure 4.5 A picture of the combustion aerosol generator (CAG).

A quench-air flow across the tip of the diffusion flame assisted in the production of highly concentrated aerosols while it also served to carry the aerosol downstream of the combustion chamber. The quenched flame exhaust was then quickly diluted using a blower to provide an ultrafine carbonaceous aerosol. Aerosol sampling was carried out using an isokinetic sampling system. The number concentration and particle size distributions can be generated by varying the air and fuel flows in the combustion chamber, the level of the flame nozzle from the top of the chamber, and the quench air flow. Stable polydisperse aerosols with particle number concentrations of approximately 10^{12} particles/m^3 were obtained (Cleary *et al.* 1992). Figure 4.5 shows a picture of the CAG. The mean particle size obtained by scanning electron microcopy was in the range between 10 – 500 nm. Figure 4.6 shows the particle morphologies of agglomerates collected obtained from the scanning electron micrograph (taken with a JEOL JSM-6335F Field Emission Scanning Electron Microscope, operated at a 15 kV and magnification of 10,000X).

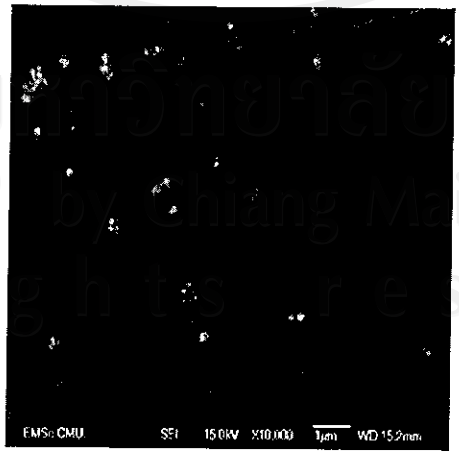

Figure 4.6 Scanning electron micrograph of the ultrafine carbonaceous particles from the CAG.

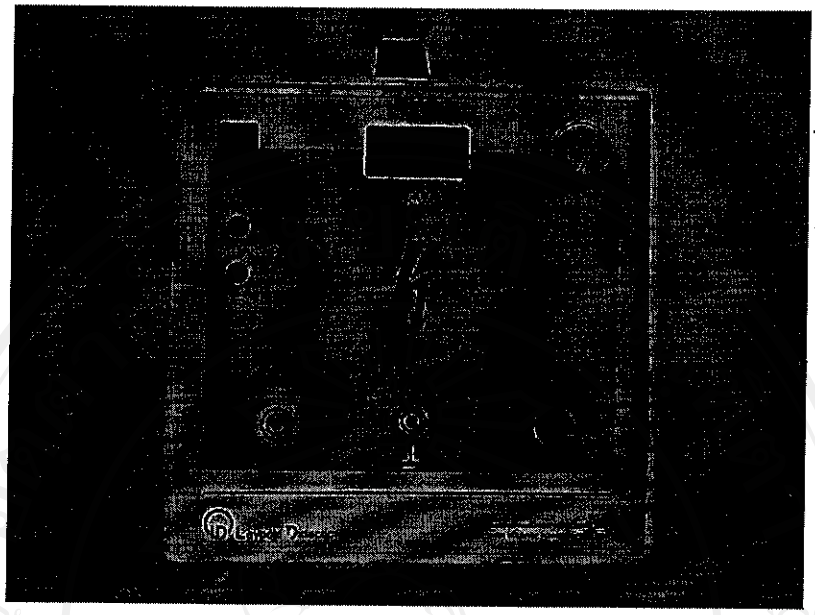

Figure 4.7 A picture of the Leybold Didactic model 521721.

4.1.4 Adjustable DC High Voltage Power Supply

An adjustable DC high voltage power supply was used to maintain the corona voltage difference in the charger and the voltage difference in the classifier column. In the present study, a commercial high voltage power supply, a Leybold Didactic model 521721, was used. In the configuration which was used, it has an output voltage range of 0 to 25 kV (potential-free), continuous, with a maximum load current of 0.5 mA, and the ripple voltage of 3 % of maximum value. A picture of a Leybold Didactic model 521721 is shown in Figure 4.7. In this study, the high voltage cable with fixed safety banana plug ends was used to connect the high voltage power supply to the charger and the classifier. The cables have a voltage rating 15,000 V with maximum current capacity is 10 A. A picture of the high voltage cable is shown in Figure 4.8.

4.1.5 Electrometer

An electrometer was used to measure the electric signal current from deposited charged particles on each electrometer ring along the inner surface of the outer electrode of the classifier column. For the present study, a commercial multi-channel electrometer, a Keithley 6517A electrometer incorporating a Keithley 6522 low current scanner card, was used. The Keithley 6517A electrometer has a special low current input amplifier with an input bias current of < 3 fA with just 0.75 fA p-p (peak-to-peak) noise, < 20 μV burden voltage on the lowest range, and the current measurement range of 1 fA to 20 mA. Figure 4.9 shows a picture of the Keithley 6517A electrometer. For the multi-channel measurement, the Keithley 6522 low current scanner card for a Keithley 6517A electrometer was used. This scanner card is a 10-channel multiplexer, has an offset current on each channel of < 1 pA and high isolation is maintained between each channel (> 10^{15} Ω). Figure 4.10 shows a picture of the Keithley 6522 low current scanner card. To avoid the leakage and noise currents, the low-noise coaxial connection cable (RG-58) was used. It has an insulation resistance of 10^{15} Ω, center conductor to shield, and contact resistance of < 0.5Ω. A picture of the low-noise coaxial connection cable is shown in Figure 4.11.

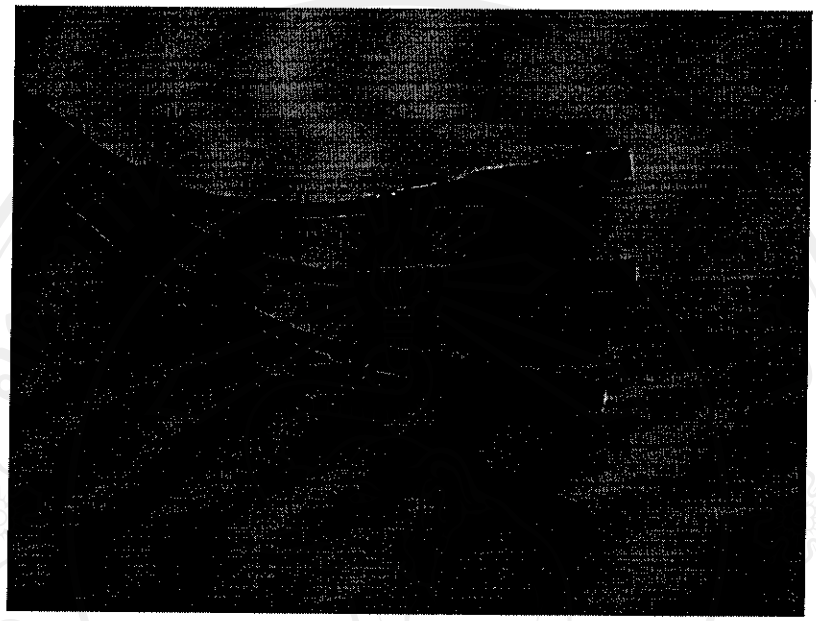

Figure 4.8 A picture of the high voltage cable.

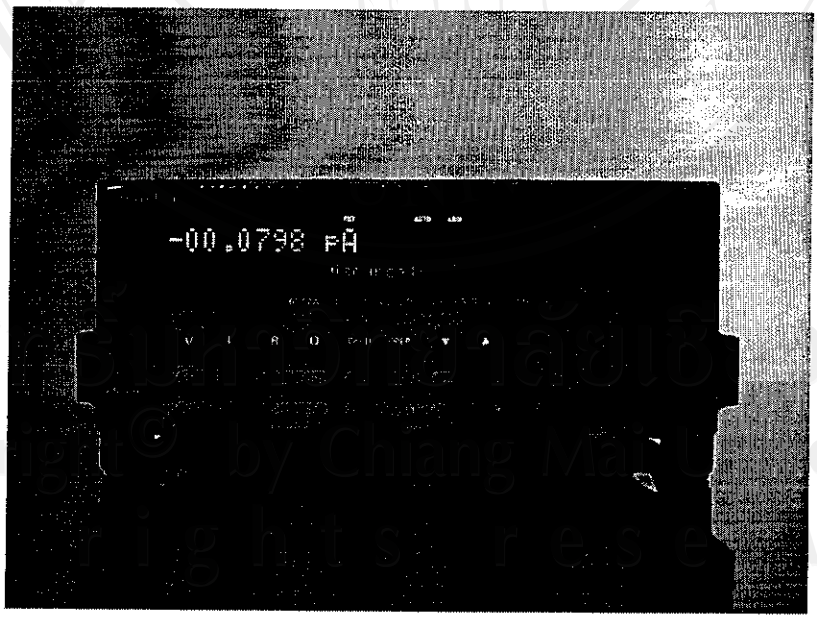

Figure 4.9 A picture of the Keithley 6517A electrometer.

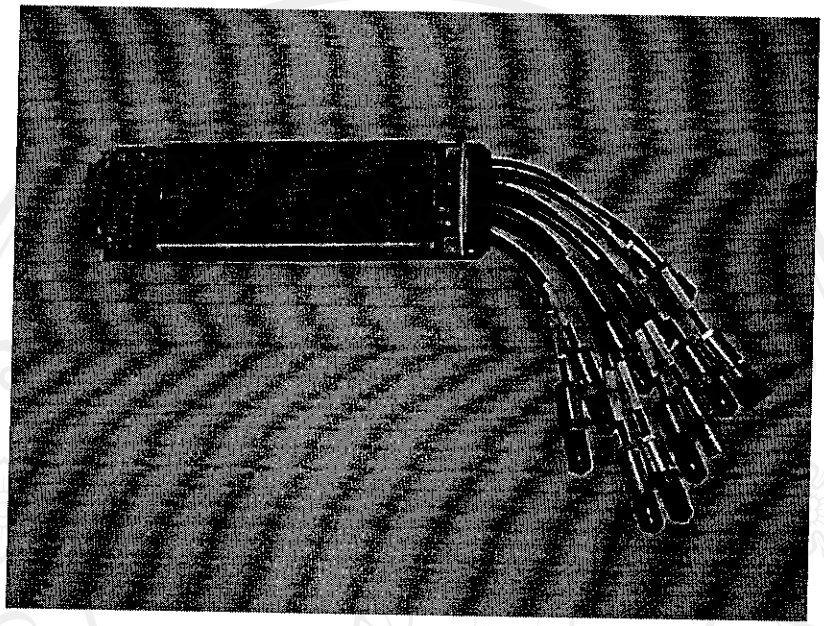

Figure 4.10 A picture of the Keithley 6522 low current scanner card.

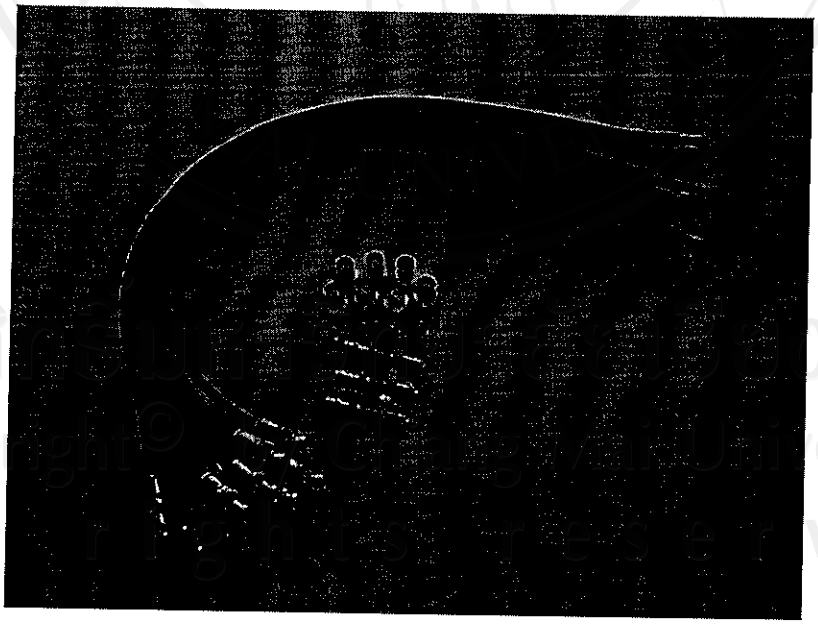

Figure 4.11 A picture of the low-noise coaxial connection cable.

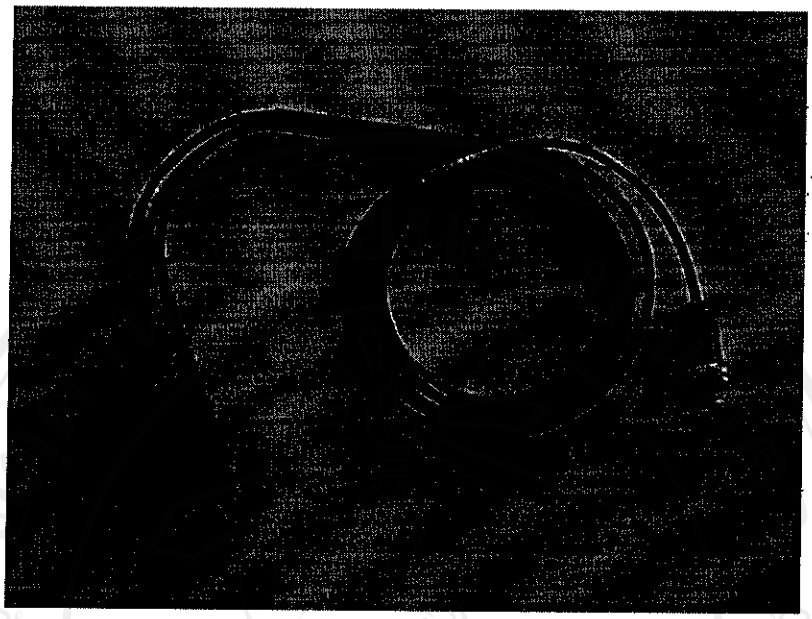

Figure 4.12 A picture of the Keithley model 237-ALG-2.

A 2-slot male triax to female BNC adapter, Keithley model 7078, was used to adapt scanner card inputs (3-lug female triax connector) to 2-lug female BNC connector and connect to the electrometer rings via a low-noise coaxial connection cable with male BNC connector on one end and spade lugs on the other 0.5 m. A 2 m of low noise triax cable terminated with a 3-slot male triax connector on one end and 3 alligator clips on the other, Keithley model 237-ALG-2, was used to connect the electrometer to the charger for measuring the charging and ionic currents. A picture of the model 237-ALG-2 is shown in Figure 4.12.

4.1.6 Scanning Electron Microscope

In this thesis, particle imaging of the collected particles inside the classifier column at each electrometer ring was carried out using a scanning electron microscope (SEM), a JEOL JSM-6335F. It is a high resolution conventional field emission scanning electron microscope. It has a resolution of 1.5 nm (5.0 nm at 1 kV), and a magnifications between 10X and 500,000X. A picture of a JEOL JSM-6335F is shown in Figure 4.13.

4.2 Experimental Procedures

This Section gives a description of the experimental arrangement and the methods used to characterize the EMS prototype.

4.2.1 Charger Evaluation

The performance of the charger is a function of the ion concentration in the charging zone, therefore continuous monitoring of the ion current from the corona-electrode to the outer electrode is necessary. The charger evaluation was carried out using the experimental setup showed in Figure 4.14. Clean dry air flow was regulated and controlled by means of a mass flow meter and controller, typically in the range between 0 – 30 l/min. The air flow was forced by a vacuum pump. An adjustable DC high voltage power supply was used to maintain the corona voltage difference, generally in the range between 1 – 10 kV.

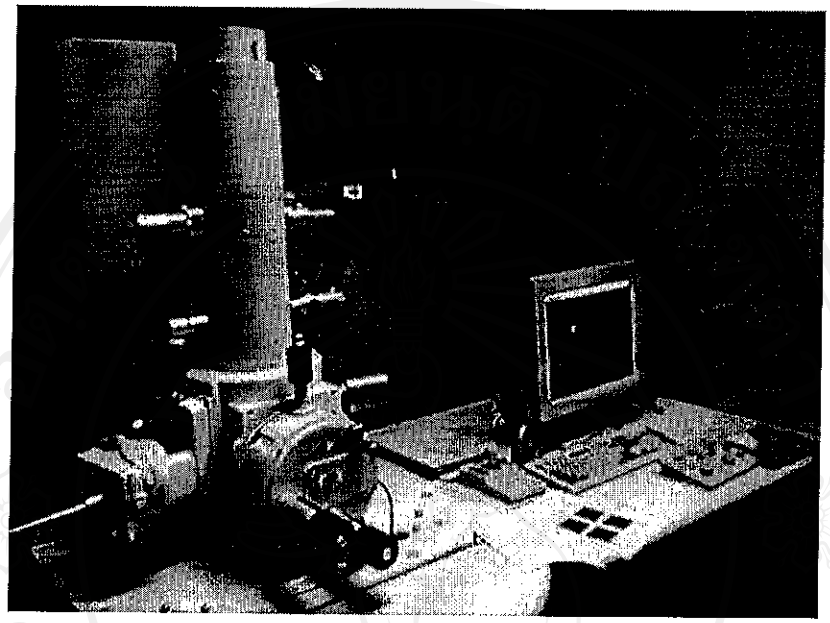

Figure 4.13 A picture of the JEOL JSM-6335F.

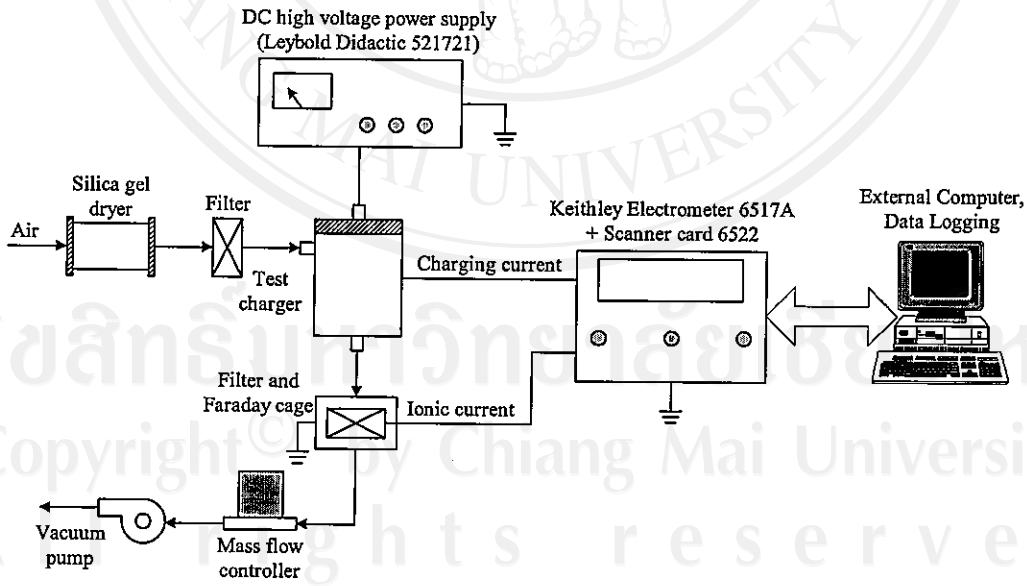

Figure 4.14 Schematic layout of the experimental setup for evaluation of the charger.

The charging current from the corona-wire electrode was measured directly with the sensitive electrometer (a Keithley 6517A electrometer incorporating a Keithley 6522 scanner card interfaced to a personal computer via an RS-232 serial port interface) via the outer electrode of the charger. It is desirable to know the ion number concentration within the charging zone, N_i, because the $N_i t$ product is the main parameter controlling the efficiency of particle charging. In this study, the ionic current at the charger outlet was measured by filtration method. An air sample was drawn into a shielded Faraday cage with a filter through which all the air passed. The filter was equipped with a fine collection metal grid, and was electrically isolated from the Faraday cage and ground. HEPA filter was used for these experiments because the collection efficiency for small air ions was very high. In the Faraday cage, the charges were removed from the air stream by the filter and the resulting ionic current flow was monitored with the sensitive electrometer. Both the charging current and ionic current were recorded by a personal computer and used for calculation of corresponding total ion number concentration. From the ionic current at the charger outlet, the ion number concentration, N_i, can be calculated from the expression

$$N_i = \frac{I_i}{eQ} \tag{4.1}$$

where I_i is the ionic current, e is the elementary charge and Q is the volumetric air flow through the filter. The ionic current measurements were translated into ion number concentrations given the total air flow rate through the charger. The ionic concentration was then used as an input for the charging models.

4.2.2 Classifier Evaluation

Figure 4.15 shows a schematic layout of the experimental setup used to evaluate the performance of the classification column. The CAG was used to generate a polydisperse carbonaceous diffusion flame aerosol for this experiment. An adjustable DC high voltage power supply was used to maintain the voltage difference between the inner and outer electrodes, typically in the range between 1.0 – 3.0 kV. The EMS was operated at aerosol flow rate in the range between 1.0 – 2.0 l/min, and pre-filtered sheath air flow rate of 10.0 l/min. In order to increase mobility resolution for particle with diameter greater than 100 nm, the EMS was maintained at sub-atmospheric pressure, typically in the range between 0.3 – 0.6 bar. The signal current from deposited charged particles on each electrometer ring was measured with a Keithley 6517A electrometer incorporating a Keithley 6522 low current scanner card, interfaced to an external personal computer via RS-232 serial port interface. Figure 4.16 shows a picture of the experimental setup of the characterization of the classification column and the overall performance of the EMS. To investigate the classification performance of the EMS, the EMS was characterized using the SEM technique.

4.2.3 SEM Analysis

In the present study, the deposited particles inside the classification column at each electrometer ring were analyzed for their size using the SEM. The sampling was carried out using a SEM copper tape 3 mm square placed on each inner surface of the electrometer ring, as shown in Figure 4.17. Aerosol samples were collected electrostatically for at least 30 minutes of operation. Particle imaging was carried out using a JEOL JSM-6335F Field Emission Scanning Electron Microscope. During the SEM analysis, agglomerates were selected and imaged randomly to minimize bias.

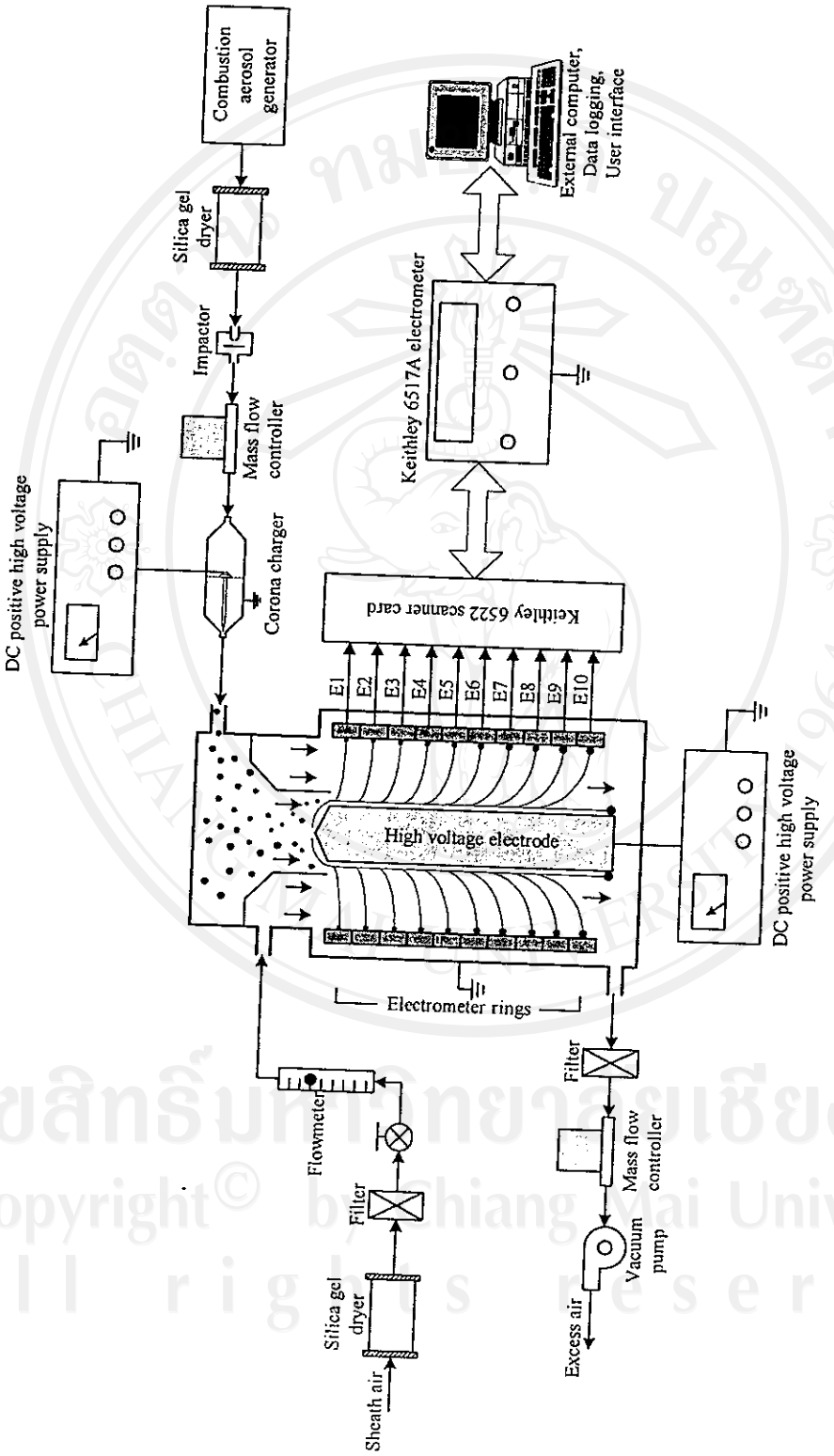

Figure 4.15 Schematic layout of the experimental setup of evaluation of the classification column and the overall performance of the EMS.

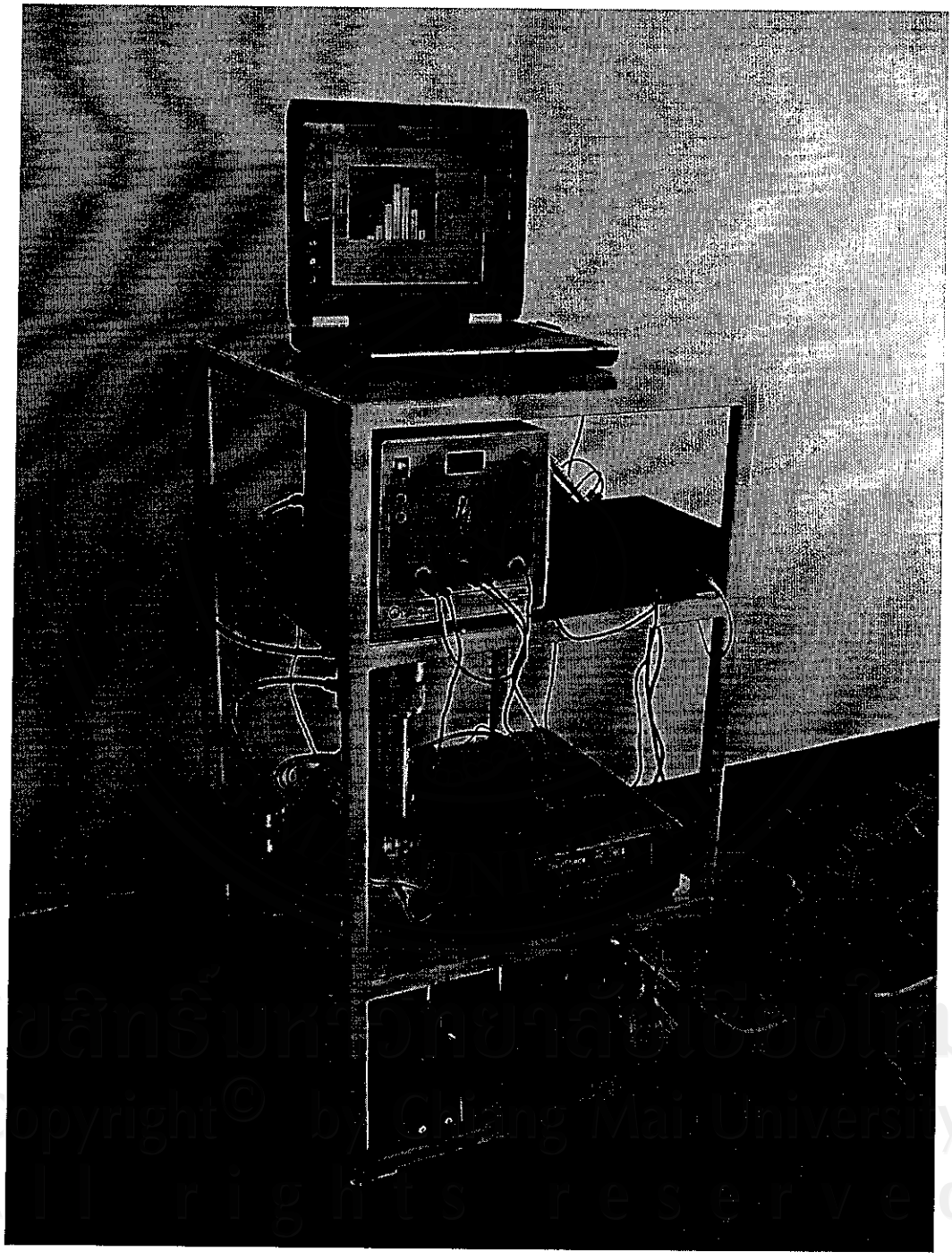

Figure 4.16 A picture of the experimental setup of the characterization of the classification column and the overall performance of the EMS.

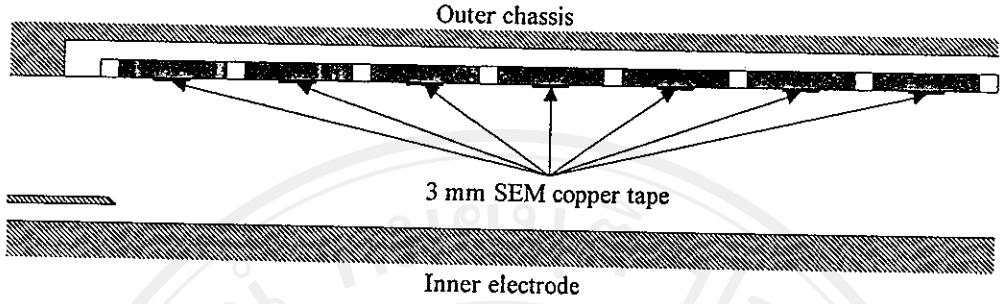

Figure 4.17 Schematic layout of the SEM sampler constructed.

Magnifications between 9,000X and 200,000X were typically used, giving two to six particles per image. For each individual sample, about 18 – 40 particle fields of view distributed throughout the sampling plate were used for SEM analysis to estimate particle surface area and determine the corresponding geometric mean projected area diameter (Ku and Maynard 2005). The SEM projected surface area distribution was obtained first, by thresholding the original SEM image and next, by calculating the projected surface area of each particle. Image processing was carried out using ImageJ processing software, a public domain JAVA image processing program which was developed at the National Institutes of Health (NIH), USA (Rasband 2004). Good image processing of the gray-level image depends on background shading and extraneous structures in the image. For this reason, the boundary of each particle was located manually before it was thresholded (Ku and Maynard 2005). The projected surface area measured from the resulting binary image varied by ± 4% due to ambiguity in the agglomerate boundary (Ku and Maynard 2005). As can be seen from Figure 4.6, a portion of the particles were found to be non-spherical and coagulated. For non-spherical or irregular shape particles, the equivalent projected surface area diameter, d_{PA}, was determined. The equivalent projected surface area diameter can be calculated from the projected surface area, A, and given by

$$d_{PA} = \sqrt{\frac{4A}{\pi}} \tag{4.2}$$

For coagulated particles, to avoid the confusion between the coagulation taking place during particle growth in the gas phase, or on the sampling plate during particle collection, the coagulated particles were excluded. It should be noted that since the sampling time is relatively short, the fraction of coagulated particles on the sampling plate was found to be small. The equivalent projected surface area diameter obtained from the SEM observations was compared with the targeted sizes calculated from the voltage applied to the classifier column. In comparison between mobility diameter and equivalent mean projected surface area diameter is similar to Rogak *et al.* (1993) and Ku and Maynard (2005).

4.2.4 Electrometer Experiments

Figure 4.18 shows the experimental setup used to evaluate the electrometer circuit performance. In this study, the electrometer circuit was calibrated with a current injection circuit (high-impedance current source). This circuit consists of an appropriately high standard resistor (10 G Ω) and an adjustable voltage source, typical in the range between 0 – 5 V. The output current, I, of this circuit can be calculated from Ohm's law, as

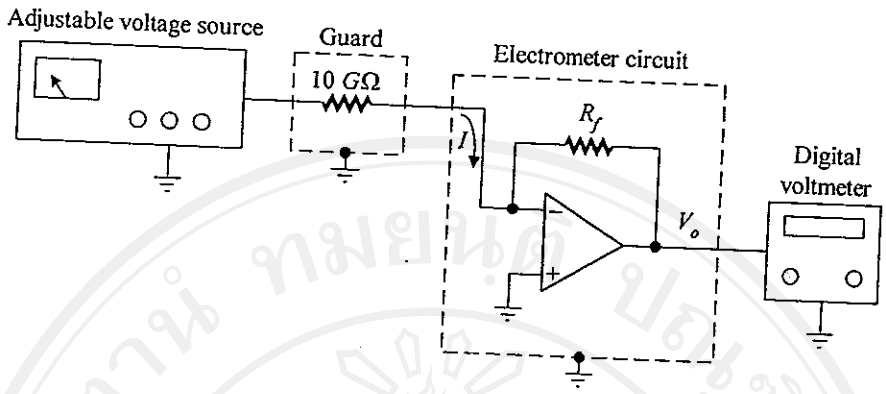

Figure 4.18 Schematic diagram of the experimental setup of the electrometer circuit calibration.

$$I = \frac{V_s}{R} \tag{4.3}$$

where V_s is the voltage source and R is the series resistor. It should be noted that the electrometer input is operated at virtual ground potential during calibration and subsequent current measurement. The output voltage from the electrometer circuit was measured and recorded by a highly accurate digital voltmeter (DVM). The voltage is then translated into the current measurements by using Equation 3.93.